Differential control of three after-hyperpolarizations in rat hippocampal neurones by intracellular calcium buffering

Alexander A. Velumian and Peter L. Carlen

Playfair Neuroscience Unit, Toronto Hospital Research Institute and University of Toronto, Toronto, Ontario, Canada M5T 2S8

(Received 1 December 1998; accepted after revision 10 February 1999)

1. The whole-cell recording technique, combined with internal perfusion, was used to study the effects of intracellular Ca^{2+} buffering on fast, medium and slow after-hyperpolarizations (fAHP, mAHP and sAHP) in hippocampal CA1 pyramidal neurones in rat brain slices at room temperature.

2. The action potentials and the fAHP were unaffected by 100 μM to 3 mM concentrations of the internally applied fast Ca^{2+} chelator BAPTA. At higher (10–15 mM) concentrations, BAPTA inhibited the fAHP and prolonged the decay of the action potential, suggesting that the corresponding large-conductance Ca^{2+}-activated K^+ channels are located close to the sites of Ca^{2+} entry during an action potential. Addition of Ca^{2+} to the BAPTA-containing solution (at a ratio of 4·5 [Ca^{2+}]: 10 [BAPTA]) to maintain the control level of $[Ca^{2+}]_i$ did not prevent the effects of high concentrations of BAPTA.

3. The mAHP, activated by a train of action potentials, was inhibited by internally applied BAPTA within the range of concentrations used (100 μM to 15 mM), and this effect could not be reversed or prevented by addition of Ca^{2+} to the BAPTA-containing solution. The inhibition of the mAHP by BAPTA could also be observed after blockade of the hyperpolarization-activated I_Q type mixed Na^+–K^+ current (also known as I_h) component of the mAHP by bath-applied 3–5 mM Cs^+, suggesting that the inhibition of the mAHP by BAPTA is due to inhibition of the depolarization-activated I_M (muscarinic) type K^+ current.

4. The sAHP, activated by a train of action potentials, was potentiated by 100–300 μM internally applied BAPTA, both with and without added Ca^{2+}. At 1–2 mM or higher concentrations, the potentiation of the sAHP by BAPTA without added Ca^{2+} was transient and was followed by a fast decrease. With added Ca^{2+}, however, BAPTA caused a persistent potentiation of the sAHP with more than a 10-fold increase in duration for periods exceeding 1 h even at concentrations of the buffer as high as 10–15 mM. Earlier reports showing a blockade of the sAHP by BAPTA, based on experiments without added Ca^{2+}, were apparently due to a sharp reduction in intracellular free [Ca^{2+}] and to a high intracellular concentration of the free buffer.

5. Internally applied BAPTA caused a prolongation of the spike discharge during an 800 ms-long depolarizing current step. At 100–300 μM BAPTA, but not at 1–2 mM or higher concentrations, this effect could be reversed by addition of Ca^{2+}. The effects of BAPTA on the spike discharge occurred in parallel with the changes in the sAHP time course, which was more prolonged at higher concentrations of the buffer.

6. The concentration-dependent differential control of the three types of AHP in hippocampal neurones by BAPTA is related to modulation of intracellular Ca^{2+} diffusion by a fast acting mobile Ca^{2+} buffer.

The after-hyperpolarization (AHP) that follows action potentials is an important intrinsic negative feedback mechanism controlling neuronal excitability. The AHP is generated by activation of distinct types of K^+ channels by Ca^{2+} ions entering the neurone during an action potential (Krnjević *et al.* 1975, 1978; Barrett & Barrett, 1976; Brown *et al.* 1990; Storm, 1990; Sah, 1996; Marrion & Tavalin, 1998). During their passage to Ca^{2+}-activated K^+ (K_{Ca}) channels, Ca^{2+} ions are subjected to various mobile and immobile intracellular Ca^{2+} buffers (Sala & Hernandez-Cruz,

1990; Nowycky & Pinter, 1993; Zhou & Neher, 1993) that can modify the intracellular Ca^{2+} dynamics and thus contribute to the AHP regulation.

In many types of neurones, the AHP consists of three distinct components: fast, medium and slow (fAHP, mAHP and sAHP). The fAHP that follows a single action potential lasts a few milliseconds and contributes to spike repolarization. The mAHP and sAHP, which have much longer durations, can also be detected following single action potentials, but are more pronounced after spike trains and play important roles in shaping the spike firing pattern. The currents generating these three AHPs, and their pharmacology, have been reviewed by Brown *et al.* (1990) and Storm (1990). The current underlying the fAHP, I_C, is generated by large-conductance channels belonging to the BK_{Ca} family that require high (1–10 μM) elevations of Ca^{2+} for their activation at negative membrane potentials, while the sAHP is generated by small-conductance (SK_{Ca}) channels that are activated by 100–400 nM Ca^{2+} (Sah, 1996). Both BK_{Ca} and SK_{Ca} channels, associated with fAHPs and sAHPs, respectively, have been recorded in hippocampal pyramidal neurones (Lancaster *et al.* 1991; Marrion & Tavalin, 1998). The mAHP exhibits a moderate Ca^{2+} dependency and is generated by three main currents: I_C, the depolarization-activated I_M (muscarinic) type K^+ current, and the hyperpolarization-activated I_Q (also known as I_h) type mixed Na^+–K^+ current (Storm, 1989, 1990).

Most studies of the effects of intracellular Ca^{2+} buffering on AHP have focused on the sAHP, showing its blockade following intracellular injection of high concentrations of EGTA or of the faster acting Ca^{2+} chelator BAPTA. These studies concluded that intracellular Ca^{2+} buffers inhibit the AHP (Krnjević *et al.* 1978; Schwartzkroin & Stafstrom, 1980; Lancaster & Nicoll, 1987; Storm, 1987*b*; Zhang & Krnjević, 1988; Lancaster & Zucker, 1994). The recent findings of *potentiating* effects of low concentrations of EGTA (Engisch *et al.* 1996) and BAPTA (Schwindt *et al.* 1992; Zhang *et al.* 1995) on the sAHP indicate the complexity of the effects of Ca^{2+} buffers.

Little and controversial data exist regarding the effects of intracellular Ca^{2+} buffering on the fAHP and mAHP. It has been reported that, in hippocampal pyramidal neurones, the spike repolarization is slowed following intracellular injection of BAPTA but not EGTA (Lancaster & Nicoll, 1987; Storm, 1987*b*), while in neocortical neurones and spinal motoneurones the effects of BAPTA on spike decay are less pronounced (Friedman & Gutnick, 1989) or absent (Krnjević *et al.* 1978; Zhang & Krnjević, 1988). The effects of chelators on the mAHP have not received much attention.

The above controversies regarding the effects of Ca^{2+} buffers on the spike shape and on the AHP are largely due to the absence of quantitative data regarding intracellular buffer concentrations. In most studies using sharp microelectrodes, the buffer concentrations in microelectrode-filling solutions were 100–200 mM or higher (e.g. Krnjević *et al.* 1978; Lancaster & Nicoll, 1987; Storm, 1987*b*; Zhang & Krnjević, 1988; Friedman & Gutnick, 1989), and only a rough guess of the intracellular buffer concentration following its diffusion or electrophoretic injection could be made (Lancaster & Nicoll, 1987). Ca^{2+} chelators in these studies were not balanced with Ca^{2+}, which could result in sharp decreases in intracellular free Ca^{2+} levels. In whole-cell recordings, patch pipette solutions often contained EGTA, BAPTA or their analogues, which may change different components of the AHP.

Based on the role of Ca^{2+} buffers in intracellular diffusion of Ca^{2+} (Sala & Hernandez-Cruz, 1990; Nowycky & Pinter, 1993), it can be proposed that the relative distance of Ca^{2+} diffusion is important in determining the possible differences in susceptibility of the fAHP and sAHP to intracellular Ca^{2+} buffers. The calculated diffusion distance for Ca^{2+} during the 1–2 ms activation time of the fAHP in hippocampal pyramidal neurones is around 0·5 μm (Lancaster & Nicoll, 1987). The close proximity of BK_{Ca} channels to Ca^{2+} channels (Marrion & Tavalin, 1998), which is in agreement with the faster time course of the fAHP, could explain the effectiveness of the faster acting Ca^{2+} buffer, BAPTA, but not EGTA, in blocking the fAHP (Lancaster & Nicoll, 1987; Storm, 1987*b*). A higher concentration of the buffer could be needed to block the fAHP, compared with the sAHP, by preventing Ca^{2+} ions from reaching the I_C-generating BK_{Ca} channels; however, this question has not been addressed so far.

Earlier studies of the effects of internally applied buffers on the AHP, whether with sharp microelectrodes or with patch pipettes, were limited in their ability to record control AHP parameters prior to buffer diffusion into the cell. In this study, we used internal perfusion of patch pipettes that allows multiple solution exchanges during recordings from a single neurone in the brain slice (Velumian *et al.* 1993). This paper shows differential, concentration-dependent effects of BAPTA on the fAHP, mAHP and sAHP.

During the first minutes of cell dialysis in whole-cell recording experiments there is an interplay between the diffusion of substances from the cell into the patch pipette (washout) and from the patch pipette into the cell (Pusch & Neher, 1988; Kay, 1992) that can profoundly alter the sAHP/I_{sAHP} (current underlying the sAHP). Thus, a facilitated washout of Ca^{2+} from the cell, due to its chelation by BAPTA or EGTA in the patch pipette, could contribute to the effects produced by these buffers (see Zhang *et al.* 1995). The decrease in $[Ca^{2+}]_i$ due to its washout or chelation by the buffer diffused into the cell could cause a potentiation of the sAHP by increasing the transmembrane Ca^{2+} gradient and hence the depolarization-evoked Ca^{2+} entry into the cells. The washout of G-proteins, causing a disinhibition of Ca^{2+} currents (Wagner & Alger, 1994), could also play a role in potentiating the sAHP/I_{sAHP}. The internal perfusion allowed us to separate the effects of internally applied substances from those of washout.

The results presented in this paper have been published previously in abstract form (Velumian & Carlen, 1997).

METHODS

Preparation

Twenty-seven- to 37-day-old male Wistar rats were decapitated under halothane (Fluothane) anaesthesia, and the brain was dissected out and cut into 400 μm-thick slices on a Vibratome-1000 in ice-cold artificial cerebrospinal fluid (ACSF). The experiments were performed in accordance with the regulations of University of Toronto and Toronto Hospital Animal Care Committee. The slices were incubated for 1–8 h in ACSF at room temperature before use.

Whole-cell recording and internal perfusion

For recording, the slices were fully submerged in a bath perfused at a rate of 3–5 ml min^{-1} at room temperature. A detailed description of the whole-cell recording and internal perfusion can be found elsewhere (Velumian *et al.* 1993, 1997). A 'blind' method of approaching neurones, based on combined pressure pulse–step movement of the pipette within the slice (Velumian *et al.* 1995), was used. The patch pipettes had outer tip diameters of 2·5–3·5 μm and resistances of 2–5 MΩ. The seal resistances before membrane rupture varied between 2 and 5 GΩ, and the access resistances after establishment of the whole-cell configuration were 2–7 MΩ.

For internal perfusion, a fine plastic tube was introduced into the patch pipette to within 250–350 μm from its tip, and solutions with different buffer concentrations were loaded immediately before use and perfused to completely replace the intrapipette solution (for details, see Velumian *et al.* 1993). To minimize junction potential changes during perfusion of different internal solutions, an agarose bridge (140 mM potassium methyl sulphate ($KMeSO_4$) or potassium gluconate and 10 mM KCl in 1% chromatographic grade agarose) was used inside the patch pipette holder (Velumian *et al.* 1997).

The effectiveness of solution replacement was tested in a few neurones, after the tests with buffer-containing solutions were completed, by changes of the action potential repolarization on replacement of internal K^+ with Cs^+ (Fig. 3*E*; caesium gluconate or $CsMeSO_3$ was used, depending on the potassium salt to be replaced). These effects, as well as the recovery upon washout of Cs^+, were complete within 3–5 min. The effects of BAPTA and EGTA developed more slowly (see Results), due to the slower diffusion of these molecules into the cells, and depended on concentration gradients. Other factors affecting the effectiveness of internal perfusion, such as the access resistance, the geometry of the patch pipette, positioning of the perfusing tube inside the patch pipette and the perfusion rate, have been discussed elsewhere (Pusch & Neher, 1988; Velumian *et al.* 1993).

The commands for current or voltage pulses applied to the neurones through patch pipettes were generated with pCLAMP software (version 5.5; Axon Instruments). The recorded signals, amplified with an Axoclamp-2A amplifier (Axon Instruments), were digitized through a 12-bit analog-to-digital interface (TL-1; Axon Instruments) and stored on an IBM PC. The data were analysed with pCLAMP/Clampfit (version 6.0; Axon Instruments). The graphs were plotted using SigmaPlot (Jandel Scientific, USA) from data quantified by pCLAMP/Clampfit.

Solutions

All internal and external solutions were prepared using deionized sterile water (specific resistance, 18·2 MΩ cm) made with the Milli-Q UV Plus system (Millipore). The chemicals used in the ACSF were purchased from Sigma. For internal solutions, most chemicals were obtained from Sigma, $KMeSO_4$ was from ICN, potassium gluconate and Hepes were from Fluka, and BAPTA (tetrapotassium salt; K_4-BAPTA) was purchased from Molecular Probes.

The standard external solution (ACSF) contained (mM): 125 NaCl, 3 KCl, 1·25 NaH_2PO_4, 2 $CaCl_2$, 2 $MgCl_2$, 26 $NaHCO_3$ and 10 D-glucose, pH 7·4 after equilibration with 95% O_2 and 5% CO_2.

The composition of the standard internal solution used for filling or perfusing the patch pipettes was (mM): 130–150 (in different experiments) $KMeSO_4$ or potassium gluconate, 10 Hepes, 0·1 EGTA and 2 K_2-ATP, pH adjusted to 7·25 with KOH. Although gluconate causes a fast rundown of the sAHP (Zhang *et al.* 1994), this effect can be reversed by internal perfusion of 1–3 mM BAPTA (Velumian *et al.* 1997). The shape of action potentials recorded with gluconate- or $MeSO_4$-based internal solutions is similar, although gluconate causes a reversible partial inhibition of the fAHP (Velumian *et al.* 1997).

K_4-BAPTA was added to the internal solution to give final concentrations varying from 100 μM to 15 mM. With K_4-BAPTA concentrations below 2 mM, no ionic substitutions were made in the internal solutions to compensate for osmolarity changes, which could result in an increase of up to 10 mosmol l^{-1}. However, the shape of action potentials and the characteristics of different components of the AHP were the same within the internal osmolarity range 270–295 mosmol l^{-1} and the $[K^+]$ range of 130–150 mM.

When higher concentrations of K_4-BAPTA are used, the increase in intracellular $[K^+]$ could affect the recorded AHPs. For example, with 15 mM K_4-BAPTA, the increase in intracellular $[K^+]$ could be as high as 60 mM, assuming a complete dissociation of the salt. Hence the concentration of $KMeSO_4$ or potassium gluconate was correspondingly reduced. Initially, a 15 mM BAPTA-containing internal solution was made by replacing 60 mM $KMeSO_4$ or potassium gluconate with 15 mM K_4-BAPTA, the calculated osmolarity change compensated by addition of 38·25 mM sucrose or mannitol, and the pH adjusted to 7·25 with KOH. Testing the osmolarity of such a 15 mM K_4-BAPTA-containing solution using a Micro-osmometer Model 3MO (Advanced Instruments Inc., USA) usually showed less than 10 mosmol l^{-1} difference from the standard internal solution, which was further compensated with appropriate amounts of sucrose or mannitol. Solutions with 5–10 mM BAPTA were made by appropriate dilutions of the above 15 mM K_4-BAPTA solution with the corresponding $KMeSO_4$- or potassium gluconate-based standard internal solution.

Two types of BAPTA-containing solutions, with and without added Ca^{2+}, were used. To calculate the free Ca^{2+} level and the amount of Ca^{2+} needed to maintain the free $[Ca^{2+}]_i$ at 100 nM, we used the computer program 'Cabuffer' developed by Dr J. Kleinschmidt (Department of Ophthalmology, New York University Medical Center, NY, USA) (available on the Internet at http://iubio.bio.indiana.edu/IUBio-Software+Data/molbio/mswin/mswin-or-dos/). Control measurements of free $[Ca^{2+}]$ were made with Dr Owen T. Jones (Playfair Neuroscience Unit, Toronto Hospital Research Institute, Toronto, Ontario, Canada) by using ratiometric fura-2 fluorescence (10 nM fura-2; excitation at 340 and 380 nm, emission at 510 nm wavelength). The calibration fluorescence curve was plotted using the Calcium Calibration Buffer Kit no. 2 from Molecular Probes. The difference between calculated and measured values for free $[Ca^{2+}]$ in the internal solutions was less than 10%.

The fura-2 fluorescence measurements showed the presence of 40–50 μM Ca^{2+} in the water used for preparing the internal solutions. Addition of 0·1 mM EGTA buffered this contaminating

Ca^{2+} to levels between 75 and 110 nM. As expected (see also Velumian *et al.* 1997), the free Ca^{2+} level was lower in the control gluconate-based internal solution (around 40 nM) than in the $KMeSO_4$-based solution (around 70 nM). Addition of BAPTA or EGTA to these solutions further decreased the free Ca^{2+} levels. Thus, with 1 mM and higher concentrations of BAPTA, the free $[Ca^{2+}]$ was reduced to levels below 5 nM. To maintain the control levels of free Ca^{2+} in BAPTA-containing solutions, Ca^{2+} was added to the internal solutions at a ratio $[Ca^{2+}]_{total}$: [BAPTA] of 4·5 : 10, which is close to previously reported values (Beech *et al.* 1991; Yu *et al.* 1994). To prepare these solutions, a stock 100 nM free Ca^{2+} buffer solution was made by adding 6·75 mM $CaCl_2$ to the 15 mM BAPTA-containing internal solution described above, and after adjusting the pH to 7·25, diluting this solution to lower BAPTA concentrations by mixing it immediately before use with a standard internal solution based on the same main salt (potassium gluconate or $KMeSO_4$). In these Ca^{2+}-balanced solutions, the free Ca^{2+} levels varied, depending on the dilution, between 53 and 70 nM in the presence of gluconate, and between 95 and 169 nM in the presence of methyl sulphate. Although no further adjustments of free $[Ca^{2+}]$ in these solutions were made, it is important to note that the effects of internally applied BAPTA, both with and without added Ca^{2+}, were observed with the use of both gluconate- and methyl sulphate-based solutions.

Experimental protocol and data analysis

Before internal perfusion of a BAPTA-containing solution, the cells were dialysed and equilibrated with the standard BAPTA-free intrapipette solution for at least 3–5 min, and control recordings were performed during the next 5–10 min. With internal solution replacement, one to three parameters were recorded repeatedly at 60 s or longer time intervals. After the effective replacement of the internal solution, which usually took 5–20 min depending on the BAPTA concentration, the set of measurements was repeated, and then the internal solution was replaced again.

The recordings included action potentials evoked by short (1–3 ms) and long (20–40 ms) depolarizing current pulses, spike trains during an 800 ms depolarizing current injection and after-potentials following the spike trains. Since the number and frequency of action potentials generated during 800 ms depolarizing pulses were affected by internal BAPTA application, a standard train of action potentials (20–40 spikes s^{-1}, 300–800 ms) activated by 1–3 ms suprathreshold current pulses was used in many experiments to analyse the effects of BAPTA on the post-spike train mAHP and sAHP. In voltage-clamp experiments (discontinuous single electrode voltage clamp; switching frequency, 3 kHz), tail currents following 200–800 ms depolarizing voltage steps from about −55 to 0 mV, which are associated with the sAHP (Brown *et al.* 1990; Storm, 1990; Caeser *et al.* 1993; Zhang *et al.* 1995), were studied.

To assess the effects of Ca^{2+} buffers, the changes in amplitude, time course and the area of AHPs were analysed. Since the control peak amplitude of sAHP/I_{sAHP} could not be measured precisely due to overlap with the response to the depolarizing command, we also measured the amplitude of control sAHP/I_{sAHP} at the same post-stimulation latency as the clearly identifiable peak of the prolonged response recorded after intracellular perfusion of Ca^{2+} buffers. To analyse the changes in the time course of the sAHP/I_{sAHP} caused by buffer perfusion, the rise time, half-width and the amplitude at different times after the depolarizing pulse and/or the latency of the peak of the response were measured. Measurement of the area of I_{sAHP} (shown in the graph of Fig. 1*A*) allowed assessment of the changes in the overall strength of the sAHP by showing the total amount of charge carried through the membrane.

For the mAHP, the peak amplitude and the area between the termination of the depolarizing pulse and the notch separating the mAHP from the sAHP (e.g. Fig. 2*B*) were measured. To analyse the effects of buffers on spike repolarization, the half-width of the action potential and the first derivative of spike decay (dV/dt) were measured.

RESULTS

Internal perfusion of BAPTA caused a concentration- and use-dependent hyperpolarization of neurones that increased with repeated activation of the sAHP. With 100–300 μM BAPTA, this hyperpolarization was less than 3 mV while with concentrations higher than 1 mM it exceeded 10–15 mV in some cells. Balancing the BAPTA with Ca^{2+} to maintain the free Ca^{2+} level (see Methods) significantly reduced this hyperpolarization. Thus, with 15 mM BAPTA balanced with 6·75 mM Ca^{2+}, the background membrane hyperpolarization did not exceed 6–7 mV.

In voltage-clamped neurones, the hyperpolarizing effect of BAPTA was manifested by an increased outward holding current (Fig. 1). In current-clamp experiments, the background hyperpolarization caused by BAPTA could affect the recorded AHPs due to their high sensitivity to membrane potential changes. To avoid this, in these experiments the membrane potential was held at a stable level throughout the recording period, mostly within ±1 mV around −60 mV, by manually controlled DC current injected into the cell.

Voltage-clamp recording of effects of buffer perfusion on the sAHP

In voltage-clamp experiments, only the current following a depolarization-induced Ca^{2+} entry and corresponding to the sAHP, I_{sAHP} (see Fig. 1), was studied. A faster I_C current that precedes the I_{sAHP} (for details, see Zhang *et al.* 1995) was not analysed due to its possible distortion by an overlapping capacitative current that follows the termination of depolarizing voltage steps.

I_{sAHP} could be potentiated and prolonged by internal perfusion of 1–3 mM BAPTA (Fig. 1*A*) or EGTA (Fig. 1*B*) even after more than 1 h of recording. The potentiating effects of BAPTA could be observed in the same cell after replacement of internal $KMeSO_4$ with potassium gluconate, as shown in Fig. 1*A* during the second hour of recording. Despite the fast rundown of the I_{sAHP} in the presence of potassium gluconate (Zhang *et al.* 1994; Velumian *et al.* 1997; compare the control currents in Fig. 1*A* and *B*), the potentiating effects of BAPTA or EGTA on the I_{sAHP} could also be observed in cells in which the recordings were started with potassium gluconate (Fig. 1*B*; see also Velumian *et al.* 1997).

With prolonged administration of 1–2 mM BAPTA, the potentiation of I_{sAHP} in many cells was transient and was followed by a fast rundown during the continued BAPTA perfusion. A potentiation of I_{sAHP}, followed by the beginning of its rundown, can be seen in the graph of Fig. 1*B* during the 8 min of perfusion of 2 mM BAPTA. The time course of

this potentiation–rundown sequence depended on the rate of diffusional exchange between the patch pipette and the cell, which was largely dependent on the access resistance. Thus, with a higher access resistance in the experiment shown in Fig. 1*A*, both effects occurred much more slowly than those in the experiment shown in Fig. 1*B*.

Internally perfused EGTA could also potentiate I_{sAHP} (Fig. 1*B*); however, the effects were less consistent (4 out of 9 cells tested) than those of BAPTA, which was effective in 58 out of 61 neurones tested. When present, the effects of EGTA developed faster than those of BAPTA (Fig. 1*B*), apparently due to its smaller molecular weight and, hence, faster diffusion into the cell. One of the main complications with the interpretation of the effects of EGTA is that, unlike BAPTA, it releases hydrogen ions when binding Ca^{2+} (Smith & Miller, 1985). For this reason, in the experiments described below we focused on the effects of BAPTA.

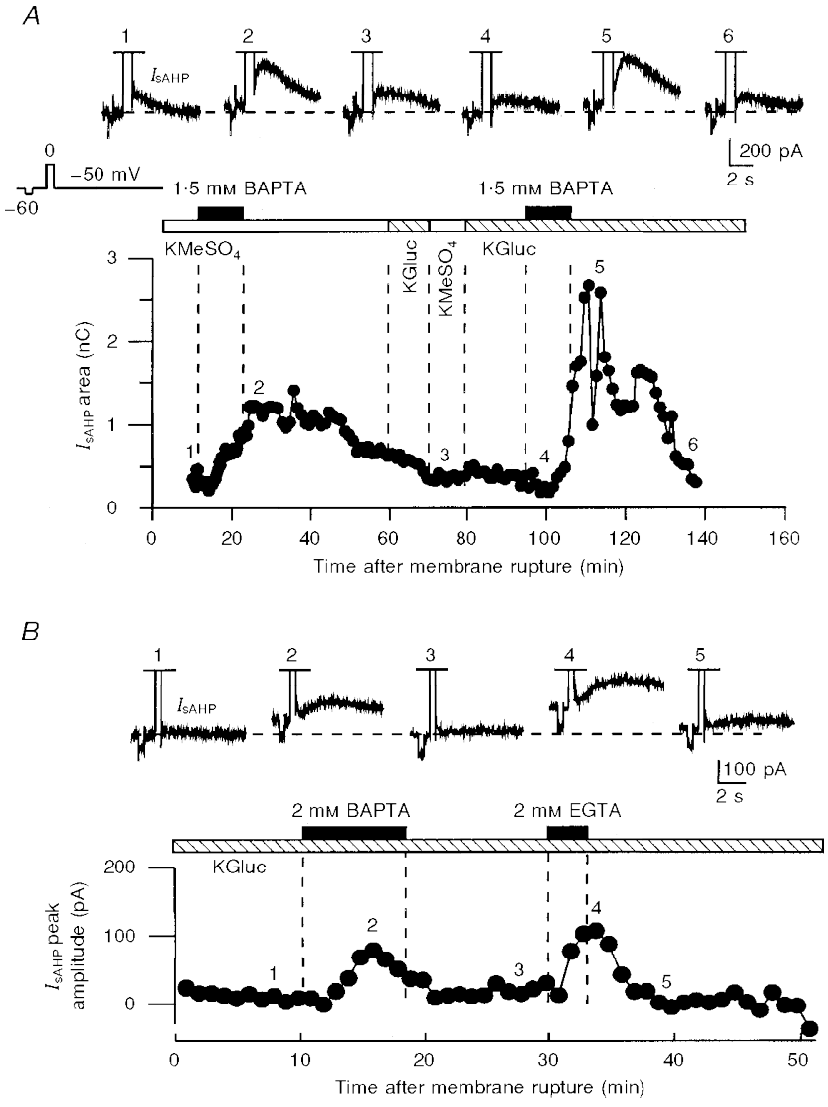

Figure 1. Potentiation of I_{sAHP} by internally perfused low millimolar concentrations of BAPTA and EGTA in two voltage-clamped neurones

A, the potentiating effects of BAPTA could be reproduced in the same neurone with both methyl sulphate- and gluconate-based internal solutions. Initially, 1·5 mM BAPTA was applied in the presence of a $KMeSO_4$-based internal solution. During the second hour of recording, after washout of BAPTA, the internal solution was replaced with a potassium gluconate-based solution (KGluc), and 1·5 mM BAPTA was applied again. *B*, effects of internally perfused 2 mM BAPTA and 2 mM EGTA in the presence of potassium gluconate-based internal solution in another neurone. In *B*, the I_{sAHP} amplitude (measured from the holding current level), but not the area, was plotted in the graph because most of the current was off the recorded time frame. The slower effects of internal perfusion in *A* were due to a higher access resistance (*A*, 15 MΩ; *B*, 6 MΩ). In *A* and *B*, the numbers above the traces correspond to the numbers on the graphs. A −10 mV voltage step from a holding voltage of −50 mV, preceding the depolarizing voltage command used for activating Ca^{2+} influx into the cells, was used for monitoring the resting membrane conductance.

Current-clamp identification of fast, medium and slow AHPs

Current-clamp experiments were preferred for the aims of this study, due to the possibility of identifying the fAHP, mAHP and sAHP.

The mAHP and sAHP following a train of action potentials were identified by their characteristic time courses (Figs 2*B* and 3*C*). The mAHP emerged as a 50–100 ms long negative peak immediately after the termination of a spike train activated by prolonged depolarization or by repetitively applied short depolarizing pulses. The sAHP that followed the mAHP was clearly separated from the mAHP by a positive notch, and had a lower amplitude and a much slower decay than the mAHP (Figs 2*B*, 3*C*, 4*A* and *B*, 5*A*, 6*A*, 7*A* and 9*B*). Typically, in the absence of BAPTA, the rising phase of the sAHP was masked by the overlapping mAHP and the preceding depolarization/spike train voltage transients, and the decay of the sAHP lasted 1–5 s. The fAHP was identified as a fast negative deflection following single action potentials (Fig. 2*A*).

Effects of internally applied BAPTA on spike frequency accommodation

With a $KMeSO_4$-based standard internal solution, neurones responded to a prolonged depolarizing pulse with a burst of action potentials followed by a period of silence (spike frequency accommodation) despite the continued depolarization (Figs 2*B* and 3*B*). This pattern, which is close to the normal firing pattern seen with sharp microelectrode studies (e.g. Lancaster & Nicoll, 1987), was not observed with potassium gluconate-based standard internal solutions which caused both a fast rundown of the sAHP and a conversion of the burst into continuous firing during the prolonged depolarizing pulse (not illustrated; see also Zhang *et al.* 1994; Velumian *et al.* 1997). During prolonged recordings with a $KMeSO_4$-based standard internal solution, the number of action potentials in the burst decreased from 4–7 to 1–3, without noticeable changes in the amplitude or time course of the sAHP. In contrast to this, internally applied BAPTA caused a dose-dependent increase in the number of action potentials generated during prolonged depolarization, as well as a prolongation of the spike discharge (Fig. 2*B*).

Since BAPTA decreases $[Ca^{2+}]_i$, we also tested the effects of restoring the control $[Ca^{2+}]_i$ by addition of appropriate amounts of Ca^{2+} to the BAPTA-containing solutions. As shown in Fig. 3*B*, addition of Ca^{2+} restored the spike firing pattern modified by 100–300 μM BAPTA ($KMeSO_4$-based internal solutions). These changes occurred in parallel with the prolongation of the rising phase of the sAHP (Fig. 3*B* and *C*). With higher BAPTA concentrations, addition of

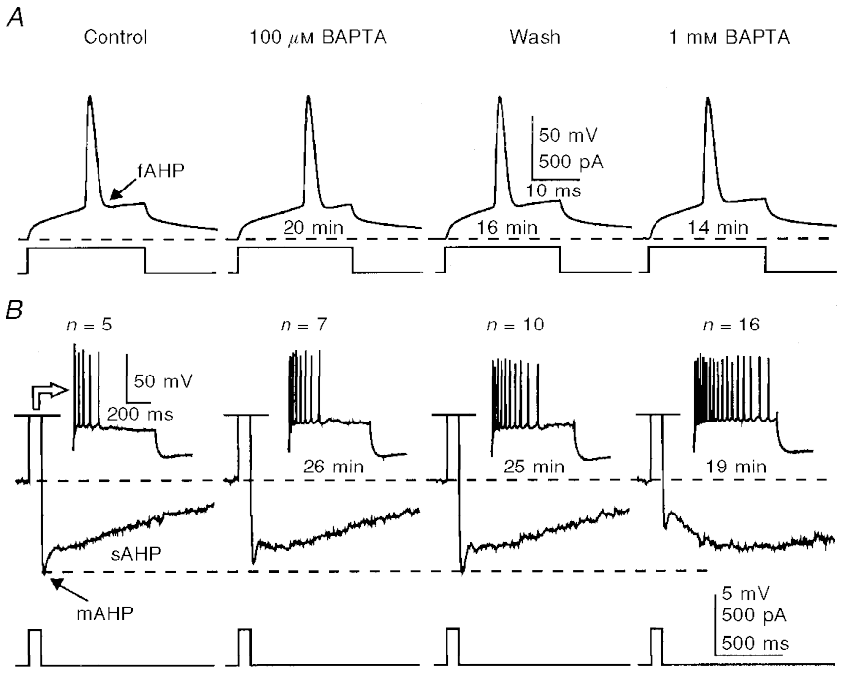

Figure 2. Potentiation of the sAHP and inhibition of the mAHP by 100 μM and 1 mM BAPTA in the same neurone

A, the amplitude and shape of action potentials did not change during perfusion of BAPTA. *B*, the mAHP/sAHP was activated by a train of action potentials generated during an 800 ms-long depolarizing current pulse. While the sAHP was potentiated, the mAHP was decreased with 100 μM and 1 mM internally applied BAPTA. Note the increase in the number (n) and frequency of action potentials generated by prolonged depolarizing pulses caused by BAPTA (insets). In *A* and *B*, the times given beneath the traces indicate the duration of internal perfusion of the solutions indicated. The membrane potential was held at −60 mV (dashed lines). $KMeSO_4$-based internal solution.

Ca^{2+} did not reverse the prolonged spike firing during depolarization (data not shown), apparently due to the slower onset and development of the sAHP.

Comparative effects of different concentrations of BAPTA on AHPs

The sAHP. As seen in Fig. 1, the rising phase of I_{sAHP}, once slowed by BAPTA, recovered very little upon subsequent washout of BAPTA, suggesting that concentrations much lower than 1–2 mM may be sufficient for prolongation of the sAHP/I_{sAHP} time course. Indeed, the time course of the sAHP could be prolonged by internal perfusion of as low as 100 μM BAPTA (Figs 2*B* and 3*C*), although the effects of these low concentrations were much less pronounced than those of 1–2 mM when compared in the same cells (Fig. 2*B*).

As shown in Fig. 3*C*, restoring the control $[Ca^{2+}]_i$ by internal perfusion of a Ca^{2+}-balanced solution of BAPTA did not

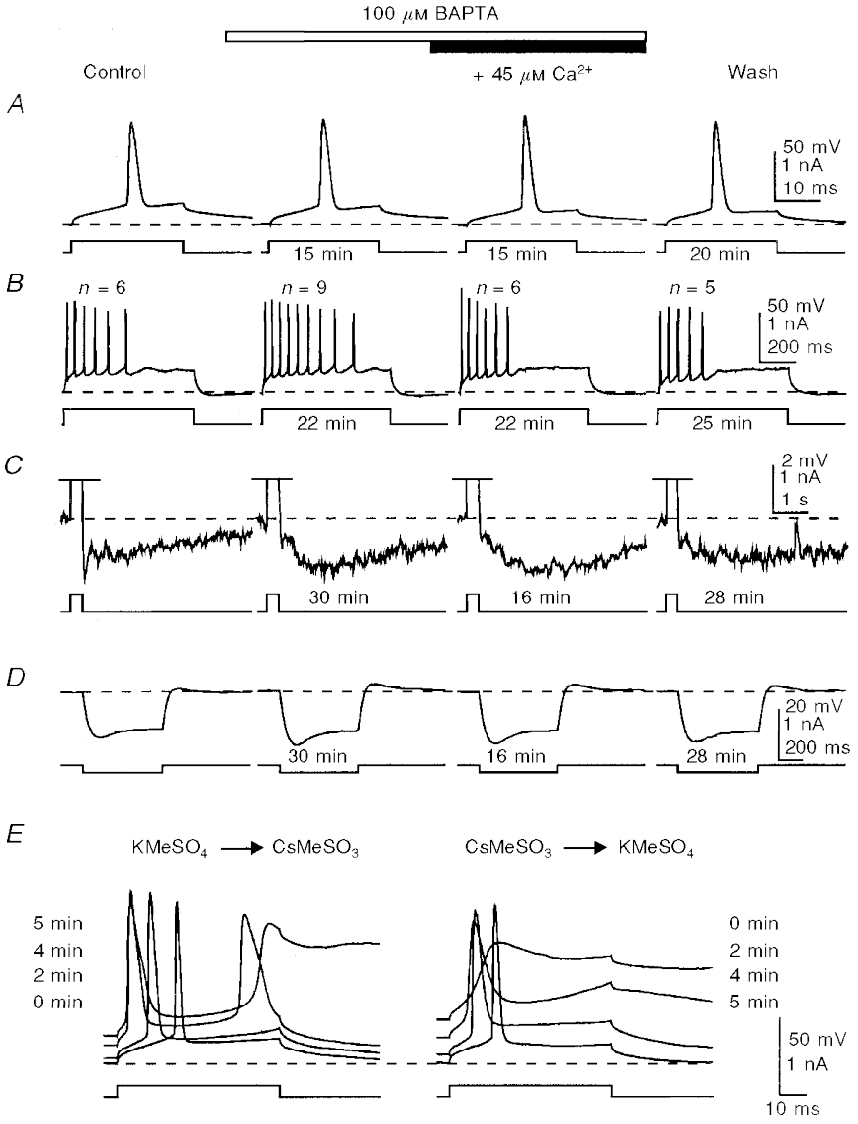

Figure 3. Addition of Ca^{2+} to restore the control $[Ca^{2+}]_i$ does not reverse the effects of submillimolar concentrations of BAPTA on the mAHP/sAHP, but does reverse the effect on spike firing pattern

The mAHP/sAHP (*C*) was activated by trains of action potentials (shown in *B*; off scale in *C*) generated during depolarizing current injections. Note the absence of BAPTA effects on the action potential (*A*) and the reduction of the mAHP during potentiation of the sAHP (*C*). At concentrations of 100–300 μM, BAPTA caused a slight increase in the membrane input resistance, as revealed by voltage responses to hyperpolarizing current steps (*D*). *E*, the effectiveness of internal perfusion was tested in this cell after washout of BAPTA by replacing internal K^+ with Cs^+ (see Methods). Note the recovery of the number of action potentials (*n*) generated by a depolarizing pulse after addition of Ca^{2+} to the BAPTA-containing solution (*B*), and a correspondence between these changes and the onset of the sAHP. The times shown indicate the duration of perfusion of a particular solution before the traces were taken. The membrane potential was held at −60 mV (dashed lines). $KMeSO_4$-based internal solution.

reverse the sAHP-prolonging effects of BAPTA. While the sAHP-prolonging effects were observed in all tested cells, only a minor (20% or less) increase in sAHP amplitude by submillimolar (100–300 μM) concentrations of BAPTA was revealed in 11 out of 16 cells perfused with BAPTA not balanced by Ca^{2+} (unchanged in 5 cells) and in 6 out of 7 cells perfused with 4·5 : 10 Ca^{2+}-balanced BAPTA (unchanged in 1 cell). One to 2 mM BAPTA caused up to a 50% temporary increase in the sAHP amplitude, i.e. much less than the 2- to 5-fold increase in the amplitude of I_{sAHP} in voltage-clamp experiments, apparently due to the attenuating effects of the increased membrane conductance during the generation of the sAHP.

As shown in Fig. 4, internal perfusion of submillimolar (Fig. 4*A*) or low millimolar (Fig. 4*B*) concentrations of BAPTA caused a potentiation of the sAHP following standard bursts of action potentials similar to that observed following long depolarizing pulses (Figs 2*B* and 3*C*). As with sAHPs activated by long depolarizing pulses, addition of Ca^{2+} to the BAPTA-containing solution did not reverse or prevent the potentiating effect of BAPTA on these sAHPs (Fig. 4*B*).

In the continued presence of 1–2 mM ($KMeSO_4$-based internal solution: $n = 17$ cells; potassium gluconate-based solution: $n = 6$ cells) or higher ($KMeSO_4$-based solution: 10 mM, $n = 4$ cells; 15 mM, $n = 4$ cells; potassium gluconate-based solution: 10 mM, $n = 3$ cells; 15 mM, $n = 4$ cells) concentrations of BAPTA and when no Ca^{2+} was added to compensate for the decrease in background free [Ca^{2+}], the potentiation of the sAHP was transient and was followed by a fast rundown (not illustrated; see also Zhang *et al.* 1995). With 10–15 mM BAPTA and no added Ca^{2+}, the sAHP potentiation–prolongation phase occurred faster than that with lower concentrations of the buffer, and with the continued presence of BAPTA the sAHP disappeared completely within 3–5 min (Fig. 5).

In contrast to the transient potentiation of the sAHP that was observed during prolonged internal perfusion of 1 mM or higher concentrations of BAPTA without added Ca^{2+}, Ca^{2+}-balanced solutions with concentrations of BAPTA as high as 10–15 mM caused a stable and long-lasting potentiation of the sAHP, and increased the total duration of the sAHP by up to 30 s or more (Figs 6 and 9; 10 mM BAPTA + 4·5 mM Ca^{2+}: $KMeSO_4$-based internal solution,

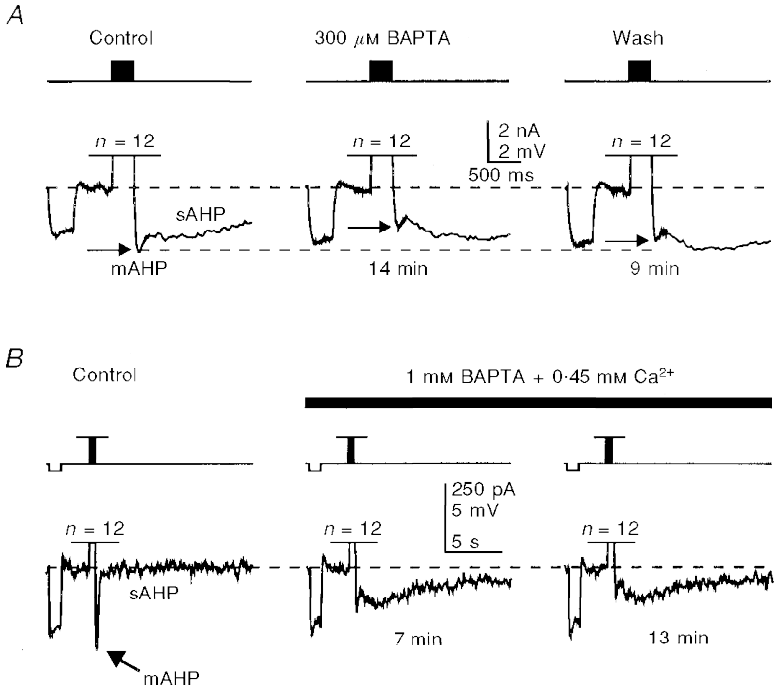

Figure 4. Internally perfused BAPTA potentiates the sAHP and inhibits the mAHP following standard spike trains activated by repetitive short (3 ms) suprathreshold current pulses in two different neurones

A, effects of internally perfused 300 μM BAPTA on the mAHP and sAHP in the presence of $KMeSO_4$-based internal solution. *B*, in another neurone, the mAHP was reduced in amplitude during BAPTA perfusion despite the increase in amplitude of the underlying sAHP, which was virtually absent in this cell due to the use of the gluconate-based internal solution, thus suggesting that the decrease of mAHP in cases such as that illustrated in *A* is not due to a decreased underlying sAHP voltage caused by the prolongation of its rising phase. Each train consisted of 12 action potentials (n) activated at a frequency of 40 spikes s^{-1}. In all traces, a 25 pA hyperpolarizing current pulse was injected into the cell prior to short pulse trains to test the membrane input resistance. The membrane potential in each cell was held at −62 mV (dashed lines). The times given beneath the traces indicate the duration of internal perfusion of the solutions indicated.

$n = 5$ cells; potassium gluconate-based solution, $n = 10$ cells; 15 mM BAPTA + 6·75 mM Ca^{2+}: $KMeSO_4$-based solution, $n = 7$ cells; potassium gluconate-based solution, $n = 8$ cells).

The mAHP. As shown in Figs 2*B*, 3*C*, 4*A* and *B*, 5*A*, 6*A*, 7*A* and 9*B*, as well as potentiating the sAHP, the internally applied BAPTA caused a profound decrease in the mAHP amplitude, varying between 15 and 85% in different neurones within the range of BAPTA concentrations used. The effects of BAPTA on the mAHP were inhibitory when both long suprathreshold depolarizing current pulses (Figs 2*B*, 3*C* and 5*A*) and standard trains of action potentials (Figs 4, 6*A*, 7*A* and 9*B*) were used to activate the mAHP/sAHP. As with the potentiating effects of low submillimolar concentrations of BAPTA on the sAHP (see above), the inhibitory effects of BAPTA on the mAHP could not be reversed by internal perfusion of BAPTA balanced with appropriate amounts of Ca^{2+} to restore the control $[Ca^{2+}]_i$ level (Fig. 3*C*). The inhibition of the mAHP could also be observed at the early stages of internal perfusion of higher concentrations of BAPTA (Fig. 5), apparently reflecting the dynamics of intracellular buffer concentration during perfusion. The mAHP amplitude decreased during both the transient potentiation of the sAHP by 10–15 mM BAPTA without added Ca^{2+} (Fig. 5*B*) and the prolonged potentiation of the sAHP by BAPTA with added Ca^{2+} to maintain the free $[Ca^{2+}]_i$ level (Fig. 6*A* (lower traces) and *B*).

The membrane input resistance was often increased by 10–30% during internal perfusion of low submillimolar concentrations of BAPTA, and this effect could not be reversed or prevented by addition of Ca^{2+} to the BAPTA-containing solution to restore the free $[Ca^{2+}]_i$ level (Figs 3*D* and 7*B*). The opposite effects of low submillimolar concentrations of BAPTA on the mAHP and sAHP suggest that the changes in amplitude of these after-potentials cannot both be due to the changes in membrane input resistance.

The blockade of I_Q (I_h) by bath-applied 3–5 mM Cs^+, which caused a 50% or more reduction of the mAHP amplitude and a sharp increase in the membrane input resistance, did not prevent the inhibitory effects of BAPTA on the mAHP (Fig. 7).

The fAHP. The fAHP does not reach an actual hyperpolarizing level in hippocampal pyramidal CA1 neurones. With action potentials activated by short (1–3 ms) depolarizing current pulses, the fAHP is overlapped by a pronounced depolarizing after-potential (DAP; Fig. 8*A*, middle and right panels) with amplitudes often exceeding 10 mV, which could obscure the full-size fAHP. Despite the differences in their ionic mechanisms (cf. Storm, 1987*a*; Azouz *et al.* 1996), the fAHP and the DAP showed a similar voltage dependence, with a 'reversal' around −45 to −50 mV (Fig. 8*A*, right panel), which is close to the spike threshold level in these neurones. As shown in Fig. 8*A*, the DAP increased in amplitude with membrane hyperpolarization and decreased with depolarization, while the fAHP became more pronounced with membrane depolarization. As shown

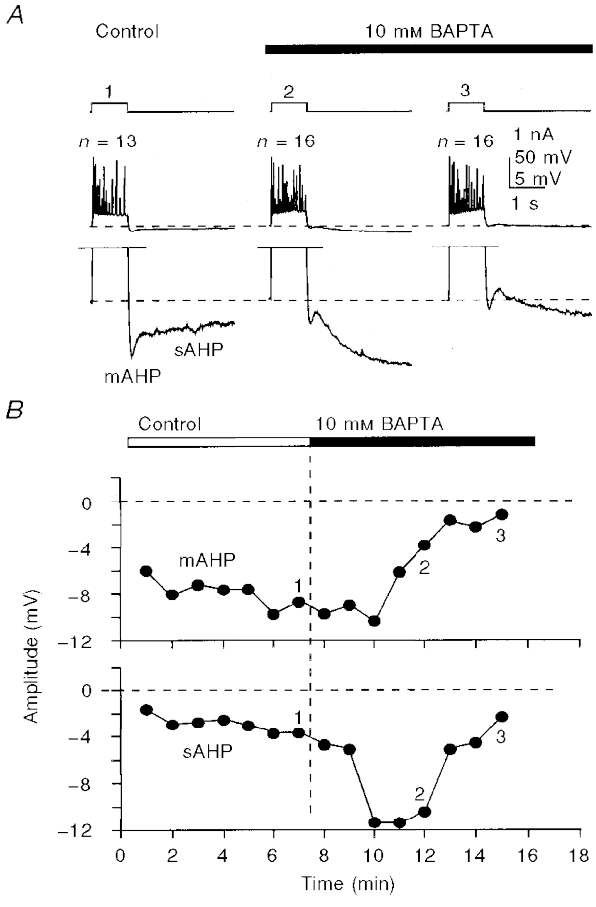

Figure 5. Transient potentiation of the sAHP and prolonged inhibition of the mAHP by internally perfused 10 mM BAPTA

A, sample responses to 400 pA, 800 ms depolarizing current pulses taken at corrresponding times shown by numbers on the graph (*B*). Note the differences in the time courses of the inhibition of the mAHP and potentiation of the sAHP during BAPTA perfusion. The appearance of a small depolarizing component separating the mAHP and the sAHP at later stages of BAPTA perfusion (*A*3) was a common phenomenon with 10–15 mM concentrations of BAPTA. The membrane potential was held at −62 mV (dashed lines in *A*). The number of action potentials (n) generated by depolarizing pulses is shown above the traces in *A*. $KMeSO_4$-based internal solution.

in the right-panel inset of Fig. 8*A*, the test for voltage dependence of the fAHP/DAP was performed with 800 ms current steps, with 1–3 ms depolarizing current pulses applied at the end of this pulse to activate an action potential.

With long (20–40 ms) depolarizing current pulses (Figs 2*A* and 3*A* and *E*), the possible distortions of the fAHP by the DAP were less obvious due to the smaller size of the DAP at depolarized membrane voltages, and the action potentials were followed by an undershooting fAHP when referred to the underlying membrane voltage. The exponential membrane voltage transients caused by depolarizing current steps complicated the precise determination of the actual size of the fAHP in these tests. To measure the actual size of the fAHP, a subthreshold voltage trace was multiplied by

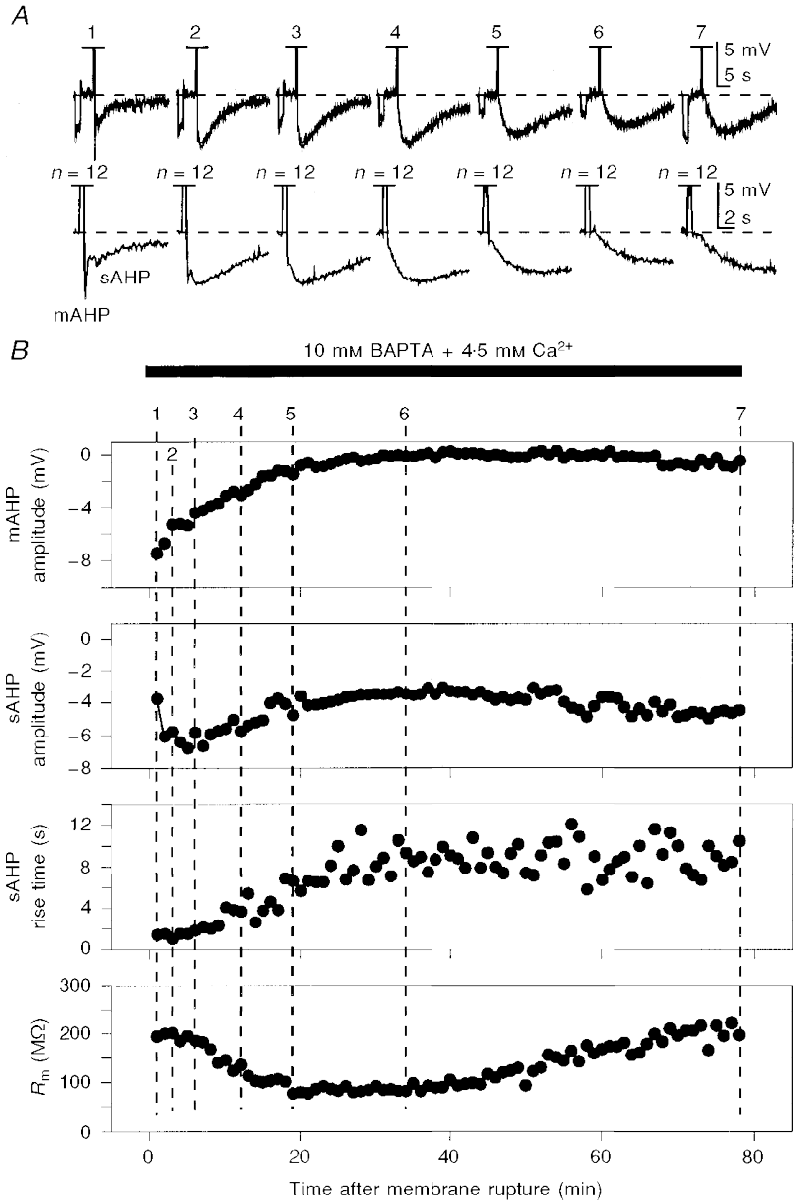

Figure 6. The time course of sAHP potentiation and mAHP inhibition during prolonged whole-cell recording with an internal solution containing 10 mM BAPTA balanced with 4·5 mM Ca^{2+}

The mAHP/sAHP was activated by standard trains of action potentials (*n*, off scale in traces shown in *A*) similar to those in Figs 5 and 7. The bottom traces in *A* show the early parts of the upper traces on an expanded time scale to show the changes in mAHP. The reponses in *A* were taken at the times indicated by the corresponding numbers on the graphs in *B*. A −25 pA current pulse was applied before the spike train (*A*) to monitor the membrane input resistance (R_m). The fluctuations of the rise time of the sAHP seen in the graph are due to possible errors introduced by the normal noise combined with the slow digitization rate, which was needed to show the full time course of these extremely slow sAHPs. The membrane potential was held at −63 mV (dashed lines in *A*). $KMeSO_4$-based internal solution.

an appropriate factor to extrapolate its size to that at the spike threshold level (Fig. 8*B*, dotted lines in upper traces), and then subtracted from the trace with an action potential (Fig. 8*B*, lower traces).

Internally applied BAPTA at concentrations up to 1 mM did not have noticeable effects on the size and shape of action potentials or the fAHP (Figs 2*A*, 3*A* and 8*B*). At concentrations of 10–15 mM, however, BAPTA reduced the speed of spike repolarization in its later half (Fig. 9*A*), which is largely contributed by the fAHP. The inhibitory effects of high BAPTA concentrations on the fAHP occurred whether or not the BAPTA was balanced with Ca^{2+} to maintain the free $[Ca^{2+}]_i$ at the normal level, and could be observed with both $KMeSO_4$- and potassium gluconate-based internal solutions (no added Ca^{2+}: $KMeSO_4$-based solution: 10 mM BAPTA, $n = 4$ cells; 15 mM BAPTA, $n = 4$ cells; potassium gluconate-based solution: 10 mM BAPTA, $n = 3$ cells; 15 mM BAPTA, $n = 4$ cells; with added Ca^{2+}: $KMeSO_4$-based solution: 10 mM BAPTA, $n = 5$ cells; 15 mM BAPTA, $n = 7$ cells; potassium gluconate-based solution: 10 mM BAPTA, $n = 10$ cells; 15 mM BAPTA, $n = 8$ cells).

DISCUSSION

The main finding of this study is that intracellular Ca^{2+} buffering by fast acting and diffusible Ca^{2+} buffers such as BAPTA has differential effects on distinct types of after-hyperpolarizations in neurones depending on the intracellular concentration of the buffer and its Ca^{2+} load.

In earlier studies, to study their effects on the AHP, Ca^{2+} buffers were applied to the cell interior through buffer-loaded sharp microelectrodes (Krnjević *et al.* 1975, 1978; Schwartzkroin & Stafstrom, 1980; Lancaster & Nicoll, 1987; Storm, 1987*b*; Zhang & Krnjević, 1988; Schwindt *et al.* 1992) and through whole-cell recording patch pipettes (Zhang *et al.* 1995; Engisch *et al.* 1996), were released intracellularly from photolabile compounds (Lancaster & Zucker, 1994) or were bath applied in an acetoxymethyl (AM) ester form (Niesen *et al.* 1991; Spigelman *et al.* 1996) which becomes active after being taken up by the cells and de-esterified. In most of these and related studies, the intracellular concentration of the buffers, as well as the Ca^{2+} load of the buffers, could not be controlled.

The use of the internal perfusion technique allows one to separate the effects of Ca^{2+} buffers applied through the patch

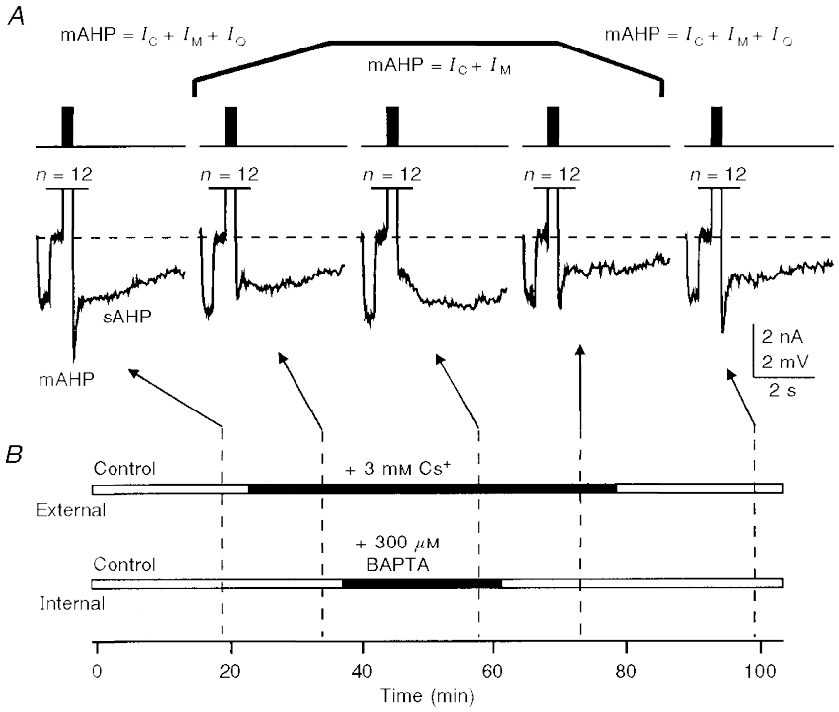

Figure 7. Inhibitory effects of submillimolar concentrations of BAPTA on the mAHP can be observed after blockade of the I_Q (also known as I_h) component of the mAHP by Cs^+ ions

A, trains of 12 action potentials (n, 40 spikes s^{-1}, 300 ms) activated by 3 ms, 1500 pA current steps, were used to induce the mAHP/sAHP. A −25 pA current pulse was applied prior to each spike train to monitor the membrane input resistance. The bar diagrams in *B* show the timing of external and internal solution replacements. Addition of 3 mM Cs^+ to the external solution reversibly blocked the hyperpolarization-activated I_Q, as manifested by the increased voltage responses to −25 pA current steps, and decreased the amplitude of the mAHP. The slight increase in membrane input resistance during internal perfusion of 300 μM BAPTA was often observed with low (100–300 μM) submillimolar BAPTA concentrations. The membrane potential was held at −62 mV (dashed lines in *A*). $KMeSO_4$-based internal solution.

pipettes from other effects that occur due to the diffusional exchange between the patch pipette and the whole-cell recorded neurone. Thus, we minimized the possible role of disinhibition of Ca^{2+} currents due to washout of G-proteins (Wagner & Alger, 1994), and ruled out the role of decreased $[Ca^{2+}]_i$ caused by BAPTA in the potentiation of the sAHP by low concentrations of the buffers.

The membrane hyperpolarization caused by intracellularly applied BAPTA in hippocampal CA1 neurones has a reversal potential close to the K^+ equilibrium potential and, similar to I_{sAHP}, can be blocked by 1 mM Ba^{2+} and 0·5–1 μM carbachol (Zhang *et al.* 1995). This hyperpolarization could be due to the enhanced tonic activation of SK_{Ca} channels by Ca^{2+} ions that were initially captured by the buffer after their depolarization-induced entry into the cell, and then subsequently released. With repeated activation of sAHPs in the presence of BAPTA, even with stimulation intervals as long as 60–90 s, there might also be an undetected summation of the sAHPs due to their increased duration caused by BAPTA. Both these mechanisms could contribute to a background activation of SK_{Ca} channels, resulting in a reduced size of the sAHPs despite prevention of an actual steady-state hyperpolarization in the cells in this study by injected currents. These mechanisms, however, are unlikely to be responsible for the increased duration of the sAHP caused by the buffer.

The importance of intracellular buffer concentration, capacity and background free Ca^{2+} level

Intracellular mobile Ca^{2+} buffers play a dual role in the dynamic control of Ca^{2+}-dependent functions. While contributing to the control level of background free $[Ca^{2+}]_i$, these buffers also exert an important shuttle function, chelating the Ca^{2+} ions at the site(s) of their elevation caused by, e.g. depolarization-induced entry into the cell, and releasing Ca^{2+} through the course of intracellular diffusion/transport to sites with lower Ca^{2+} levels (Schwindt *et al.* 1992; Zhou & Neher, 1993; Zhang *et al.* 1995).

While the effects of intracellular Ca^{2+} buffers in the dynamic control of the AHP depend greatly on the Ca^{2+}-binding kinetics of the buffer (discussed by Zhang *et al.* 1995), the efficacy of mobile buffers both in maintaining the free $[Ca^{2+}]_i$ level and in shuttling the Ca^{2+} ions within the cell may vary depending on the free buffer concentration or, more specifically, on its Ca^{2+}-binding capacity, which may increase or decrease depending on topographic variations of $[Ca^{2+}]_i$.

The potentiation of the sAHP by low concentrations of internally applied BAPTA is attributed to prolongation of the intracellular Ca^{2+} signal following depolarization-induced Ca^{2+} entry into the cell (Sala & Hernandez-Cruz, 1990; Schwindt *et al.* 1992; Nowycky & Pinter, 1993; Zhang *et al.* 1995). In the first publication on this phenomenon in neurones (Schwindt *et al.* 1992), based on internal administration of BAPTA and analogues *without* added Ca^{2+}, it was also assumed that the effects of the buffers were due to the reduction of background intracellular free Ca^{2+} concentration. Our present findings that the potentiation of the sAHP by BAPTA also occurs when the reduction of intracellular free $[Ca^{2+}]$ is prevented or reversed by using Ca^{2+}-balanced buffer solutions, rules out this explanation

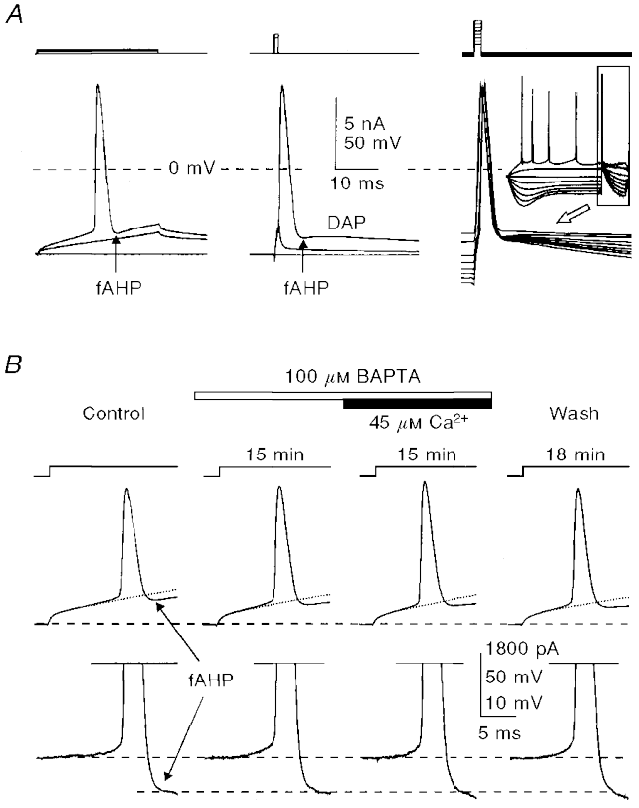

Figure 8. Submillimolar concentrations of BAPTA do not affect the size and shape of action potentials and the amplitude of the fAHP both without and with added Ca^{2+}

A, comparison of fAHPs following action potentials activated by long (left) and short (middle and right) depolarizing current pulses. *B*, separation of the fAHP (recorded in the cell shown in Fig. 3) by digital subtraction of the normalized subthreshold voltage transient (shown with dotted lines on upper traces) from the traces with action potentials, the results of which are shown in the lower traces. The times given indicate the duration of internal perfusion of the particular solutions indicated. The membrane potential was held at −60 mV (dashed lines). $KMeSO_4$-based internal solution.

and favours the mechanism based on a slowed decay of the Ca^{2+} signal. According to this mechanism, the successive influxes of Ca^{2+} may summate with the BAPTA-prolonged tails of preceding $[Ca^{2+}]_i$ signals, thus bringing the transient elevations of $[Ca^{2+}]_i$ to greater-than-normal values (Schwindt *et al.* 1992). Apparently, maintaining the background free $[Ca^{2+}]_i$ by adding proper amounts of Ca^{2+} to buffer-containing solutions would help to maintain the normal 'tuning' levels of the different K^+ channels involved in the generation of distinct types of AHP.

Concentration-dependent effects of internally applied BAPTA on the sAHP

As mentioned in the Introduction, the quantitative aspect of the intracellular BAPTA or EGTA load could not be addressed in most of the earlier studies performed with sharp microelectrodes. The calculated intracellular buffer concentration achieved with 200 mM buffer-containing microelectrodes, based on a comparison with IPSP-reversing Cl^- diffusion from the microelectrode into the cell, was around 7 mM (Lancaster & Nicoll, 1987). This concentration is close to the concentrations found in our study to inhibit the fAHP (10–15 mM), but is far above the submillimolar concentrations that cause a steady potentiation of the sAHP when no Ca^{2+} is added. Due to differences in diffusibility, permeation and membrane transport between Cl^- and BAPTA, however, the above estimate may not be correct. The effects of lower intracellular concentrations of chelators, which could occur at early stages of diffusion of the buffers into the cells, may have been overlooked in many sharp microelectrode studies due to the usual delay in the onset of recordings to allow the membrane potential to stabilize after microelectrode penetration.

As shown more recently with low-resistance (10–12 MΩ) sharp microelectrodes (Schwindt *et al.* 1992) and with whole-cell recordings (Zhang *et al.* 1995; Engisch *et al.* 1996), and confirmed in this study, 1–2 mM concentrations of internally applied BAPTA or EGTA, when not balanced with Ca^{2+}, can cause only a temporary potentiation of the sAHP/I_{sAHP} followed by its complete blockade. Balancing 1 mM BAPTA or EGTA in the patch pipette solution with amounts of Ca^{2+} varying from a ratio of 1 : 10 (Zhang *et al.* 1995; Engisch *et al.* 1996) to 1 : 1 (Zhang *et al.* 1995) prolongs the duration of the sAHP/I_{sAHP} potentiation period, delaying the subsequent blockade of sAHP/I_{sAHP}. According to our data, a 4·5 : 10 ratio instead of the widely used 1 : 10 $[Ca^{2+}]$:[BAPTA] ratio should be used to maintain the free $[Ca^{2+}]$ at a level of 100 nM. With this ratio, the sAHP recorded in neurones, using either $KMeSO_4$- or potassium gluconate-based internal solutions, persists for more than an hour with concentrations of BAPTA as high as 10–15 mM, its time course being prolonged in a buffer concentration-dependent manner.

The potentiation of the sAHP/I_{sAHP} by internally applied BAPTA occurs at buffer concentrations as low as 100 μM (see also Zhang *et al.* 1995; Spigelman *et al.* 1996). This concentration could even be lower, since, as shown in this study, loading the buffer with 45 μM Ca^{2+}, which would reduce the free BAPTA concentration, did not reverse the sAHP-prolonging effects of the buffer. Our estimates, based on the buffer concentration in the patch pipette, show only

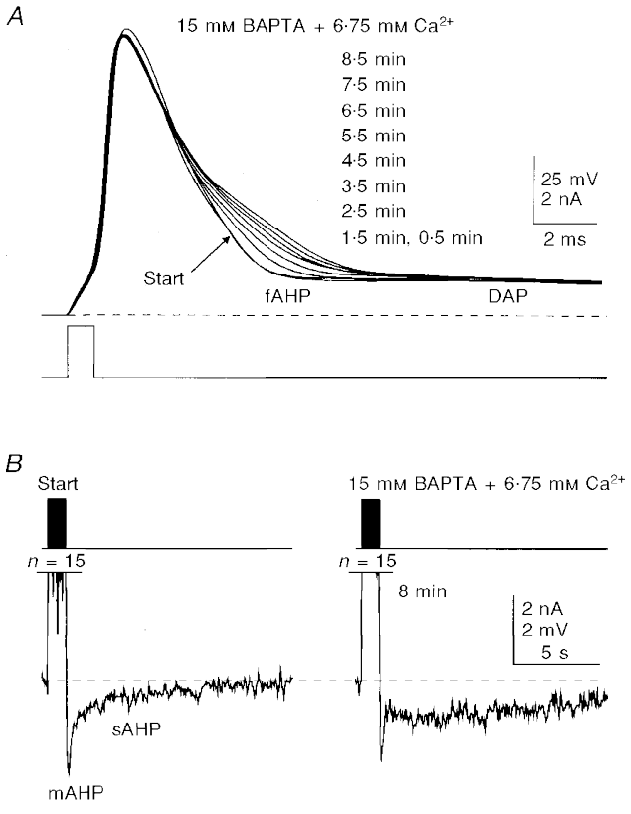

Figure 9. Blockade of the fAHP and prolongation of the action potential decay with Ca^{2+}-balanced 15 mM BAPTA

In this cell, the whole-cell recording was started with a patch pipette loaded with 15 mM BAPTA. *A*, prolongation of the second half of the decay of the action potential caused by BAPTA. *B*, in the same cell, the mAHP/sAHP showed changes that were qualitatively similar to those observed at lower BAPTA concentrations. Inhibition of the mAHP seen in *B* began before the trace marked Start was recorded (0·5 min after establishing the whole-cell recording configuration) due to the possible faster diffusion of BAPTA into the cell caused by a very high concentration gradient. The membrane potential was held at −62 mV (dashed lines). Potassium gluconate-based internal solution. *n*, number of action potentials. The times shown indicate the duration of internal perfusion of the BAPTA solution before the traces were taken.

the upper possible limit of buffer concentration in the cell, which could be much lower due to the limited rate of diffusional exchange between the patch pipette and the cell interior (Pusch & Neher, 1988) and the extrusion of BAPTA from the cells by organic anion pumps (Ouanounou *et al.* 1996).

Based on the effects of different concentrations of BAPTA, a bell-shaped dependence of the sAHP amplitude on intracellular BAPTA concentration without added Ca^{2+} can be predicted with a peak between 0·3 and 1 mM. The initial increase in the sAHP amplitude at early stages of diffusional exchange between the high BAPTA-loaded patch pipette and the cell (Figs 5 and 6) agrees qualitatively with this prediction. Our study further shows that balancing the buffer with Ca^{2+} to maintain the free $[Ca^{2+}]_i$ level within the physiological range significantly extends the upper limit of the sAHP-potentiating buffer concentration.

Inhibition of the mAHP by submillimolar [BAPTA]

Internally applied BAPTA, at the same concentrations which potentiated the sAHP, i.e. between 100 μM and 1 mM, caused a significant reduction of the mAHP, which could not be reversed by balancing the BAPTA with Ca^{2+} to maintain the free $[Ca^{2+}]_i$ at 100 nM. Furthermore, the inhibitory effects of submillimolar [BAPTA] on the mAHP could be observed in our experiments after blockade of one of the three main components of the mAHP, the hyperpolarization-activated inward rectifier I_Q (also known as I_h; see Storm, 1989, 1990; Brown *et al.* 1990), by bath-applied Cs^+ ions. The possible effects of submillimolar, and even low (1–3 mM) millimolar, BAPTA concentrations on another component of the mAHP, the I_C, which is also one of the main currents underlying the generation of the fAHP (Storm, 1987*a*, 1990; Lancaster & Nicoll, 1987), could be ruled out in our experiments, since spike repolarization and the fAHP were not affected by these concentrations of internally applied BAPTA. It has been shown that the contribution of I_C to the mAHP is minimal at membrane resting and hyperpolarized levels, and plays a role only at depolarized membrane potentials (Storm, 1989; Williamson & Alger, 1990). Thus, the inhibition of the mAHP by submillimolar and low millimolar concentrations of BAPTA is due to inhibition of the third known component of the mAHP, the M-type K^+ current, I_M (Storm, 1989, 1990). I_M, a voltage- and time-dependent K^+ current that is suppressed by muscarinic receptor activation (Brown *et al.* 1990; Marrion *et al.* 1991; Beech *et al.* 1991; Yu *et al.* 1994) was shown in other types of neurones to be suppressed by internal perfusion of BAPTA. However, this effect occurred at much higher concentrations of the buffer, 11–20 mM (whole-cell recording: Beech *et al.* 1991; Yu *et al.* 1994). Although a direct action of BAPTA on the M-channel at these concentrations could not be ruled out, the suppression of I_M through modulation of intracellular free Ca^{2+}, to which this current shows an indirect dependence, was proposed (Marrion *et al.* 1991; Beech *et al.* 1991; Yu *et al.* 1994).

Inhibition of the fAHP by high millimolar concentrations of BAPTA

Broadening of the action potential and a reduction of the fAHP have been reported in hippocampal pyramidal neurones impaled with 200 mM BAPTA- but not EGTA-containing microelectrodes (Lancaster & Nicoll, 1987; Storm, 1987*b*). While the preferential effects of BAPTA over EGTA in blocking the fAHP were explained in these studies by its much faster Ca^{2+}-binding kinetics, the concentration factor could not be quantitatively assessed, although a 7 mM intracellular concentration of the buffer was calculated (Lancaster & Nicoll, 1987; but see criticism above). As shown in this study, only relatively high millimolar concentrations of BAPTA (10–15 mM) can effectively block the fAHP.

As mentioned in the Introduction, the need for a Ca^{2+} buffer faster than EGTA, such as BAPTA, to block the spike repolarization and the fAHP (Lancaster & Nicoll, 1987; Storm, 1987*b*) is due to the close proximity of BK_{Ca} channels to Ca^{2+} entry sites (Marrion & Tavalin, 1998), which is also in agreement with the fast time course of the fAHP. The higher Ca^{2+} levels needed at negative membrane potentials for activation of charybdotoxin-sensitive BK_{Ca} channels that underlie I_C and the fAHP generation, as compared with SK_{Ca} channels that are responsible for sAHP generation (Lancaster *et al.* 1991), also favour the close proximity of fAHP-generating BK_{Ca} channels to Ca^{2+} entry sites. This strategic location would allow a brief exposure of I_C/fAHP-generating channels to sufficiently high elevations of $[Ca^{2+}]_i$ following single action potentials. A close and regularly arranged apposition of Ca^{2+} channels and charybdotoxin-biotin-labelled BK_{Ca} channels was shown in the presynaptic terminal of the frog neuromuscular junction (Robitaille *et al.* 1993). Our data showing that much higher concentrations of BAPTA are needed to block the fAHP, compared with the slower types of AHPs, also strongly supports the closer apposition of high-voltage-activated Ca^{2+} channels and BK_{Ca} channels in hippocampal pyramidal neurones.

Functional significance of differential control of different types of after-hyperpolarizations by intracellular Ca^{2+} buffering

Contrary to the widespread belief that fast intracellular Ca^{2+} buffers block Ca^{2+}-activated conductances and clamp the intracellular Ca^{2+} levels, it is becoming evident that, depending on buffer capacity, mobility and Ca^{2+}-binding kinetics (Sala & Hernandez-Cruz, 1990; Nowycky & Pinter, 1993; Zhou & Neher, 1993), these buffers have a more diversified role in the dynamic control of different Ca^{2+}-activated and Ca^{2+}-dependent functions in neurones (Schwindt *et al.* 1992; Zhang *et al.* 1995). Although we used an exogenous Ca^{2+} chelator, BAPTA, to study the possible mechanisms of control of the different components of the AHP, the following considerations may also apply to naturally occurring intracellular buffers.

In the differential control of the three types of after-hyperpolarization, which control the neuronal excitability over a

short time scale following single or bursts of action potentials, the role of intracellular Ca^{2+} buffers should be considered with respect to the specific roles of different types of after-hyperpolarizations, which are well classified (Storm, 1990; Sah, 1996). By prolonging the time course of the sAHP, low concentrations of fast and mobile (diffusible) buffers can have two major effects: (i) a prolongation of the spike discharge due to a delayed onset of the sAHP and (ii) longer lasting periods of silence and a decreased responsiveness of neurones following spike trains. Inhibition of the mAHP that starts at low concentrations of the buffers, but can be seen over a wide range of buffer concentrations, can contribute to the precise shaping of the spike bursts and to burst termination. A blockade of the sAHP by higher concentrations of the buffers can lead to a transformation of the depolarization-induced spike firing pattern from short bursts into a continuous firing activity, also supported by an inhibition of I_M that slowly develops during prolonged membrane depolarization and contributes to termination of the burst of action potentials. Finally, the blockade of the fAHP by very high buffer concentrations can only be expected in pathological conditions causing a marked overproduction of intracellular Ca^{2+} buffers. This picture can be further diversified by consideration of activity-dependent changes of the Ca^{2+}-buffering capacity due to an interplay between the elevations of intracellular Ca^{2+} from intra- and extracellular sources, Ca^{2+} extrusion/sequestration, and the Ca^{2+} buffering and intracellular transport by mobile buffers.

Azouz, R., Jensen, M. S. & Yaari, Y. (1996). Ionic basis of spike after-depolarization and burst generation in adult rat hippocampal CA1 pyramidal cells. *Journal of Physiology* **492**, 211–223.

Barrett, E. F. & Barret, J. N. (1976). Separation of two voltage-sensitive potassium currents, and demonstration of a tetrodotoxin-resistant calcium current in frog motoneurones. *Journal of Physiology* **255**, 737–774.

Beech, D. J., Bernheim, L., Mathie, A. & Hille, B. (1991). Intracellular Ca^{2+} buffers disrupt muscarinic suppression of Ca^{2+} current and M current in rat sympathetic neurons. *Proceedings of the National Academy of Sciences of the USA* **88**, 652–656.

Brown, D. A., Gähwiler, B. H., Griffith, W. H. & Halliwell, J. V. (1990). Membrane currents in hippocampal neurons. *Progress in Brain Research* **83**, 141–160.

Caeser, M., Brown, D. A., Gähwiler, B. H. & Knöpfel, T. (1993). Characterization of a calcium-dependent current generating a slow afterdepolarization of CA3 pyramidal cells in rat hippocampal slice cultures. *European Journal of Neuroscience* **5**, 560–569.

Engisch, K. L., Wagner, J. J. & Alger, B. E. (1996). Whole-cell voltage-clamp investigation of the role of PKC in muscarinic inhibition of IAHP in rat CA1 hippocampal neurons. *Hippocampus* **2**, 183–191.

Friedman, A. & Gutnick, M. J. (1989). Intracellular calcium and control of burst generation in neurons of guinea-pig neocortex in vitro. *European Journal of Neuroscience* **1**, 374–381.

Kay, A. R. (1992). An intracellular medium formulary. *Journal of Neuroscience Methods* **44**, 91–100.

Krnjević, K., Puil, E. & Werman, R. (1975). Evidence for Ca^{2+}-activated K^+ conductance in cat spinal motoneurons from intracellular EGTA injections. *Canadian Journal of Physiology and Pharmacology* **53**, 1214–1218.

Krnjević, K., Puil, E. & Werman R. (1978). EGTA and motoneuronal after-potentials. *Journal of Physiology* **275**, 199–223.

Lancaster, B. & Nicoll, R. A. (1987). Properties of two calcium-activated hyperpolarizations in rat hippocampal neurones. *Journal of Physiology* **389**, 187–203.

Lancaster, B., Nicoll, R. A. & Perkel, D. J. (1991). Calcium activates two types of potassium channels in rat hippocampal neurons in culture. *Journal of Neuroscience* **11**, 23–30.

Lancaster, B. & Zucker, R. S. (1994). Photolytic manipulation of Ca^{2+} and the time course of slow, Ca^{2+}-activated K^+ current in rat hippocampal neurones. *Journal of Physiology* **475**, 229–239.

Marrion, N. V. & Tavalin, S. J. (1998). Selective activation of Ca^{2+}-activated K^+ channels by co-localized Ca^{2+} channels in hippocampal neurons. *Nature* **395**, 900–905.

Marrion, N. V., Zucker, R. S., Marsh, S. J. & Adams, P. R. (1991). Modulation of M-current by intracellular Ca^{2+}. *Neuron* **6**, 533–545.

Niesen, C., Charlton, M. P. & Carlen, P. L. (1991). Postsynaptic and presynaptic effects of the calcium chelator BAPTA on synaptic transmission in rat hippocampal dentate granule neurons. *Brain Research* **555**, 319–325.

Nowycky, M. C. & Pinter, M. J. (1993). Time courses of calcium and calcium-bound buffers following calcium influx in a model cell. *Biophysical Journal* **64**, 77–91.

Ouanounou, A., Zhang, L., Tymianski, M., Charlton, M. P., Wallace, M. C. & Carlen, P. L. (1996). Accumulation and extrusion of permeant Ca^{2+} chelators in attenuation of synaptic transmission at hippocampal CA1 neurons. *Neuroscience* **75**, 99–109.

Pusch, M. & Neher, E. (1988). Rates of diffusional exchange between small cells and a measuring patch pipette. *Pflügers Archiv* **411**, 204–211.

Robitaille, R., Garcia, M. L., Kaczorowski, G. J. & Charlton, M. P. (1993). Functional colocalization of calcium and calcium-gated potassium channels in control of transmitter release. *Neuron* **11**, 645–655.

Sah, P. (1996). Ca^{2+}-activated K^+ currents in neurones: types, physiological roles and modulation. *Trends in Neurosciences* **4**, 150–154.

Sala, F. & Hernandez-Cruz, A. (1990). Calcium diffusion modelling in a spherical neuron. Relevance of buffering properties. *Biophysical Journal* **57**, 313–324.

Schwartzkroin, P. A. & Stafstrom, C. E. (1980). Effects of EGTA on the calcium-activated afterhyperpolarization in hippocampal CA3 pyramidal cells. *Science* **210**, 1125–1126.

Schwindt, P. C., Spain, W. J. & Crill, W. E. (1992). Effects of intracellular calcium chelation on voltage-dependent and calcium-dependent currents in cat neocortical neurons. *Neuroscience* **47**, 571–578.

Smith, G. L. & Miller, D. J. (1985). Potentiometric measurement of the stoichiometric and apparent affinity constants of EGTA for protons and divalent cations including calcium. *Biochimica et Biophysica Acta* **839**, 287–299.

Spigelman, I., Tymianski, M., Wallace, C. M., Carlen, P. L. & Velumian, A. A. (1996). Modulation of hippocampal synaptic transmission by low concentrations of cell-permeant Ca^{2+} chelators: effects of Ca^{2+} affinity, chelator structure and binding kinetics. *Neuroscience* **75**, 559–572.

Storm, J. F. (1987*a*). Action potential repolarization and a fast after-hyperpolarization in rat hippocampal pyramidal cells. *Journal of Physiology* **385**, 733–759.

Storm, J. F. (1987*b*). Intracellular injection of a Ca^{2+} chelator inhibits spike repolarization in hippocampal neurons. *Brain Research* **435**, 387–392.

Storm, J. F. (1989). An after-hyperpolarization of medium duration in rat hippocampal pyramidal cells. *Journal of Physiology* **409**, 171–190.

Storm, J. F. (1990). Potassium currents in hippocampal pyramidal cells. *Progress in Brain Research* **83**, 161–187.

Velumian, A. A. & Carlen, P. L. (1997). Differential effects of BAPTA on three components of the afterhyperpolarization in rat hippocampal CA1 neurons. *Society for Neuroscience Abstracts* **23**, 1747.

Velumian, A. A., Thirlwell, C. J. & Carlen, P. L. (1995). Adapters for combined intrapipette pressure pulses and patch pipette step movements during 'blind' cell search in brain slices. *Journal of Neuroscience Methods* **62**, 129–134.

Velumian, A. A., Zhang, L. & Carlen, P. L. (1993). A simple method for internal perfusion of mammalian central nervous system neurones in brain slices with multiple solution changes. *Journal of Neuroscience Methods* **48**, 131–139.

Velumian, A. A., Zhang, L., Pennefather, P. & Carlen, P. L. (1997). Reversible inhibition of I_K, I_{AHP}, I_h and I_{Ca} currents by internally applied gluconate in rat hippocampal pyramidal neurones. *Pflügers Archiv* **433**, 343–350.

Wagner, J. J. & Alger, B. E. (1994). GTP modulates run-up of whole-cell Ca^{2+} channel current in a Ca^{2+}-dependent manner. *Journal of Neurophysiology* **71**, 814–816.

Williamson, A. & Alger, B. E. (1990). Characterization of an early afterhyperpolarization after a brief train of action potentials in rat hippocampal neurons in vitro. *Journal of Neurophysiology* **63**, 72–81.

Yu, S. P., O'Malley, D. M. & Adams, P. R. (1994). Regulation of M current by intracellular calcium in bullfrog sympathetic ganglion neurons. *Journal of Neuroscience* **14**, 3487–3499.

Zhang, L. & Krnjević, K. (1988). Intracellular injection of Ca^{2+} chelator does not affect spike repolarization of cat spinal motoneurons. *Brain Research* **462**, 174–180.

Zhang, L., Pennefather, P., Velumian, A., Tymianski, M., Charlton, M. & Carlen, P. L. (1995). Potentiation of a slow Ca^{2+}-dependent K^+ current by intracellular Ca^{2+} chelators in hippocampal CA1 neurons of rat brain slices. *Journal of Neurophysiology* **74**, 2225–2241.

Zhang, L., Weiner, J. L., Valiante, T. A., Velumian, A. A., Watson, P. L., Jahromi, S. S., Schertzer, S., Pennefather, P. & Carlen, P. L. (1994). Whole-cell recording of the Ca^{2+}-dependent slow afterhyperpolarization in hippocampal neurones: effects of internally applied anions. *Pflügers Archiv* **426**, 247–253.

Zhou, Z. & Neher, E. (1993). Mobile and immobile calcium buffers in bovine adrenal chromaffin cells. *Journal of Physiology* **469**, 245–273.

Acknowledgements

We thank Dr Owen T. Jones for fura-2 fluorescence measurements of free Ca^{2+} in the internal solutions, and Mr Frank Vidic for most valuable assistance with the electronics and computers.

Corresponding author

A. A. Velumian: Playfair Neuroscience Unit, Room 12-413, Toronto Hospital Western Division, 399 Bathurst Street, Toronto, Ontario, Canada M5T 2S8.

Email: velumian@playfair.utoronto.ca